BMP4 Promotes Formation of Primitive Vascular Networks in Human Embryonic Stem Cell–Derived Embryoid Bodies

N. L. Boyd,* S. K. Dhara,* R. Rekaya,† E. A. Godbey,* K. Hasneen,* R. R. Rao,‡ F. D. West III,* B. A. Gerwe,* and S. L. Stice*,†,§,[1]

*Regenerative Bioscience Center, University of Georgia, Athens, Georgia 30602; †Animal and Dairy Science Department, University of Georgia, Athens, Georgia 30602; ‡Chemical & Life Science Engineering, Virginia Commonwealth University, Richmond, Virginia 23284; and §Georgia Tech/Emory Center for the Engineering of Living Tissues, Georgia Institute of Technology, Atlanta, Georgia 30332

The vasculature develops primarily through two processes, vasculogenesis and angiogenesis. Although much work has been published on angiogenesis, less is known of the mechanisms regulating the *de novo* formation of the vasculature commonly called vasculogenesis. Human embryonic stem cells (hESC) have the capability to produce all of the cells of the body and have been used as *in vitro* models to study the molecular signals controlling differentiation and vessel assembly. One such regulatory molecule is bone morphogenetic protein-4 (BMP4), which is required for mesoderm formation and vascular/hematopoietic specification in several species. However, hESC grown in feeder-free conditions and treated with BMP4 differentiate into a cellular phenotype highly expressing a trophoblast gene profile. Therefore, it is unclear what role, if any, BMP4 plays in regulating vascular development in hESC. Here we show in two National Institutes of Health–registered hESC lines (BG02 and WA09) cultured on a 3D substrate of Matrigel in endothelial cell growth medium–2 that the addition of BMP4 (100 ng/ml) for 3 days significantly increases the formation and outgrowth of a network of cells reminiscent of capillary-like structures formed by mature endothelial cells ($P < 0.05$). Analysis of the expression of 45 genes by quantitative real time–polymerase chain reaction on a low-density array of the entire culture indicates a rapid and significant downregulation of pluripotent and most ectodermal markers with a general upregulation of endoderm, mesoderm, and endothelial markers. Of the genes assayed, *BMPR2* and *RUNX1* were differentially affected by exposure to BMP4 in both cell lines. Immunocytochemistry indicates the morphological structures formed were negative for the mature endothelial markers CD31 and CD146 as well as the neural marker SOX2, yet positive for the early vascular markers of endothelium (KDR, NESTIN) and smooth muscle cells (α-smooth muscle actin [αSMA]). Together, these data suggest BMP4 can enhance the formation and outgrowth of an immature vascular system. Exp Biol Med 232:833–843, 2007

Key words: human embryonic stem cell; vasculogenesis; bone morphogenetic protein-4

Introduction

Vasculogenesis and angiogenesis are widely perceived as two key processes contributing to the development of the vasculature (1). Vasculogenesis comprises the formation of the earliest vessels and hematopoietic precursors from the mesodermal germ layer while angiogenesis involves the sprouting of new vessels from the established vasculature. Angiogenesis has been well studied for its therapeutic roles in blood supply regulation, wound healing, and anti-cancer treatments. However, the early events regulating vasculogenesis are relatively unknown. Many nonhuman models have been used to gain insight into vascular development; however, with the isolation of human embryonic stem cells (hESC), this process can be tested in cells of human embryonic origin.

Embryonic stem cells form embryoid bodies (EB), which can recapitulate the development of the three germ layers (ectoderm, mesoderm, and endoderm) as well as early vascular events (2–4). It has been shown in several animal models that the vasculature arises from the mesodermal germ layer (5). One of the regulatory signals instrumental in mesoderm formation is bone morphogenetic protein-4

This work was supported with funding from the Georgia Tech/Emory Center for the Engineering of Living Tissues, Georgia Research Alliance (S.L.S.), and the National Institutes of Health Kirschstein Postdoctoral Fellowship (N.L.B.).

[1] To whom correspondence should be addressed at University of Georgia, Regenerative Bioscience Center, Rhodes Animal and Dairy Science Center, 425 River Road, Athens, GA 30602. E-mail: sstice@uga.edu

Received December 1, 2006.
Accepted January 31, 2007.

1535-3702/07/2326-0833$15.00

(BMP4). Disruption of BMP4 is embryonic lethal (6). It has been shown to influence dorso-ventral body pattern (6, 7), vascular and hematopoietic development (8–10), apoptosis (11, 12), and bone formation (13). In hESC culture, BMP4 has been shown to initiate differentiation, while blocking its activity with Noggin, a BMP-signaling inhibitor, preserves pluripotence (14). It was also demonstrated that hESC grown in feeder-free conditions predominantly formed trophoblast marker expressing cells when exposed to BMP4 (15). However, it is unclear what role BMP4 plays in development of the early human vasculature.

Here we show hESC grown on Matrigel in endothelial growth medium (EGM)-2 form more extensive primitive vascular-like network structures when treated with 100 ng/ml of BMP4. These network structures are negative for the mature endothelial markers CD31 and CD146 but positive for the early vascular markers KDR, NESTIN, and smooth muscle cells (α-smooth muscle actin [αSMA]). These results indicate hESC-derived progenitor cells are capable of forming a primitive vascular complex and modeling vasculogenesis.

Materials and Methods

Cell Culture. Human embryonic stem cell lines BG02 (Bresagen, Athens, GA) and WA09 (WiCell, Madison, WI)) were cultured in Dulbecco's minimal essential medium/Ham's F12 medium (DMEM/F12), 2 m*M* L-glutamine, 0.1 m*M* minimal essential medium (MEM) nonessential amino acids, 50 U/ml penicillin, 50 μg/ml streptomycin (all from Gibco, Gaithersburg, MD), 4 ng/ml basic fibroblast growth factor (bFGF; R&D Systems, Minneapolis, MN) and 15% fetal bovine serum (FBS; Hyclone, Logan, UT), 5% knock-out serum replacement (KSR, Invitrogen, Carlsbad, CA) with 10 ng/ml leukemia inhibitory factor (LIF; Chemicon, Temecula, CA) or 20% KSR, respectively, as previously described (16, 17). Cells were cultured on mitomycin-C (Sigma Chemical Co., St. Louis, MO) mitotically inactivated murine embryonic fibroblasts, manually dissociated, and passaged to new feeder layers every 4–5 days (16).

Differentiation Procedure. Stem cell colonies were manually dissociated into aggregates of approximately 100–500 cells and transferred to tissue culture dishes containing 500 μm–thick Matrigel (BD Biosciences, Bedford, MA) formed according to the manufacturer's instructions. Cell aggregates were cultured in EGM-2 (Cambrex, Walkersville, MD) supplemented with 100 ng/ml recombinant human BMP4 (rhBMP4) (R&D Systems) or an equal volume of solvent as control (4m*M* hydrochloric acid, 0.1% bovine serum albumin [BSA] in phosphate buffered saline [PBS]) for 3 days, after which the cells were cultured in EGM-2 alone for another 5 days.

Noggin Inhibition. hESC were grown as previously described and cultured with BMP4 control and Noggin control (PBS + 0.1% BSA), 100 ng/ml BMP4, and Noggin control or 100 ng/ml BMP4 and 300 ng/ml Noggin (rmNoggin, R&D Systems) for 3 days, when supplementation ended and cells were cultured for another 3 days in EGM-2 alone.

Cellular Outgrowth Network Quantification. Phase contrast images (Nikon, Melville, NY) were acquired on a daily basis over the 8-day experiment. Day 6 images were used for quantifying the total cellular network per image field at ×4 magnification. For BG02 and WA09, five and four independent experiments, respectively, were quantified. Total cellular extensions per field were measured by using Photoshop software (Adobe, San Jose, CA), and the statistical difference between means was calculated by using a one-tailed Student's t test. Differences were considered significant at $P < 0.05$.

Gene Expression and Statistical Analysis. hESC were grown as described over an 8-day period. Samples were collected for RNA analysis on Days 0, 2, 4, 6, and 8. Total RNA was isolated using a Qiagen RNeasy kit (Valencia, CA) according to the manufacturer's instructions, and the integrity of the RNA produced from all used samples was verified and quantified by a RNA 6000 Nano Assay and the Agilent 2100 Bioanalyzer (Agilent Technologies, Santa Clara, CA). cDNA was reverse transcribed by using Superscript II (Invitrogen). For quantitative real time–polymerase chain reaction (qRT-PCR), a low-density array was custom designed by Applied Biosystems (ABI, Foster City, CA) for 47 primer sets plus an 18S endogenous control. The 47 primer sets included gene markers for pluripotence (10); the three germ layers (ectoderm [5], mesoderm [14], and endoderm [3]); and endothelial (6), trophoblast (2), and miscellaneous markers (7) (Table 1). The qRT-PCR low-density array was processed using an ABI 7900HT system. Relative quantification of the gene expression output was performed using Sequence Detection System software (SDS version 2.2.1, ABI). The SDS utilizes relative quantification of gene expression by way of the comparative C_T method where the relative quantity $(RQ) = 2^{-\Delta\Delta C_T}$, where

$$\Delta\Delta C_T = (C_{T,\text{target}} 2\ C_{T,18S})_{\text{time}} \times 2(C_{T,\text{target}} 2\ C_{T,18S})_{\text{time 0}}$$

and C_T is defined as the threshold cycle where the target gene surpasses a defined amplification (18). All genes were normalized to 18S as a loading control and with Day 0 as the base expression. The RQ was analyzed using the generalized linear model (GLM) procedure of SAS (SAS Institute, Cary, NC). The statistical model included the independent effects of BMP4 treatment, time, and the interaction between treatment and time, indicated in the text as "treatment*time". Additionally, least square means (LSMEANS) of the interaction effects and the contrasts between the two treatment levels at the five different time points were tested using Student's t test (SAS Institute, Cary, NC). The gene expression response was analyzed separately for each cell line.

Fluorescence Microscopy. Cultures were prepared and grown on Lab-Tek II glass chamber slides (Nalgene-

Nunc, Naperville, IL) on mouse embryonic fibroblasts (MEF) or glass-bottom dishes (Wilco, Bioscience Tools, San Diego, CA) as previously described. On Days 6–8, the cells were prepared for immunostaining on Matrigel by using a modified protocol described by Debnath *et al*. (19). Briefly, cultures were washed once with PBS, fixed with 4% paraformaldehyde for 20 mins at room temperature, permeablized with 0.5% Triton X-100 in PBS for 10 mins at room temperature, washed 3 times with PBS for 10 mins each, incubated with blocker (0.1% BSA and 6% secondary antibody-matched serum in PBS) for 1 hr at room temperature, incubated with primary antibody in blocker for 1 hr at room temperature or overnight at 4°C, washed with blocker 3 times for 20 mins each, incubated with secondary antibody in PBS for 1 hr, washed 3 times for 20 mins each with PBS, counterstained with diamidino-2-phenylindoline (DAPI, 1:10,000 in water; Sigma Chemical) for 5 mins at room temperature, washed once with PBS, preserved with mounting medium, and sealed with a coverslip. Antibodies used for immunocytochemistry were Oct4 (Santa Cruz Biotechnology, Santa Cruz, CA), CD31 (Chemicon, Temecula, CA, MAB2148), CD146-PE (BD Biosciences, 550315), SOX2 (R&D Systems, MAB2018), KDR (Cell Signaling, Beverly, MA, 2479), αSMA (Abcam, Cambridge, MA, AB7817) and NESTIN (Neuromics, Edina, MN MO15012). Secondary antibodies were AlexaFluor 488 goat anti-rabbit and AlexaFluor 594 donkey anti-mouse (Invitrogen-Molecular Probes, Eugene, OR) and DAPI nuclear staining (Sigma Chemical). Imaging was performed using an Olympus inverted fluorescence microscope (IX81, Center Valley, PA) with a disc-spinning unit (DSU). A series of images were collected in the Z plane and deconvolved, and a two-dimensional projection was rendered using SlideBook software version 4.1 (Intelligent Imaging Innovations, Denver, CO).

Results

BMP4 Regulates Cellular Network Outgrowth from Embryoid Bodies. To determine the effect of BMP4 in vascular development, BG02 or WA09 hESC were manually passaged as cell aggregates onto a three-dimensional Matrigel substrate in EGM-2 supplemented with either 100 ng/ml of BMP4 or control. The dose of BMP4 was chosen to correspond with that used in an earlier hESC study (15). BMP4 or control was added to fresh culture medium daily for 3 days, then supplementation was stopped and the EGM-2 was changed daily for the remaining 5 days. Supplementation was stopped after 3 days, which roughly corresponded to the initial outgrowth of network structures. The cell aggregates formed adherent spheroids reminiscent of embryoid body (EB) structures (1 day postpassage; Fig. 1). The compact EB was maintained for 2–3 days when cells began to migrate out of the EB, either along the surface or invading the gel. Typically on Days 3 to 4, the BG02 untreated cultures began to show the

Table 1. Quantitative Real Time-PCR Genes[a]

Variable	Full name
Pluripotency	
CCNA2	Cyclin A2
DNMT3B	DNA (cytosine-5)-methyltransferase 3β
EBAF	Lefty-2; left-right determination factor-2
FGF2	Fibroblast growth factor-2
FGF4	Fibroblast growth factor-4
FGFR4	Fibroblast growth factor receptor-4
FOXA2	Forkhead box A2
Oct4/POU5F1	POU domain, class 5, transcription factor-1
SALL2	EGFR, epidermal growth factor receptor
SOX2	SRY (sex determining region Y) box 2
Mesoderm	
ACVR1B	Activin-like receptor-1B
ACVR1C	Activin-like receptor-1C
BMP4	Bone morphogenic protein-4
BMPR2	Bone morphogenic protein receptor-2
CD34	Hematopoietic progenitor cell antigen CD34
CD45	PTPRC, protein tyrosine phosphatase, receptor type C
FLT1	VEGF receptor 1
FLK1/KDR	VEGF receptor 2
GATA4	GATA-binding protein 4
GSC	Goosecoid
RUNX1	Runt-related transcription factor 1
T	Brachyury
NKX2–5	NK2 transcription factor related, locus 5 (*Drosophila*)
Ectoderm	
FGF5	Fibroblast growth factor-5
FN1	Fibronectin-1
MSI1	Musashi-1
NEFH	Early neural marker; forebrain marker
NES	Nestin
Endoderm	
AFP	α-Fetoprotein
CER1	Cerberus-1
HNF4	Hepatocyte nuclear factor-4
NODAL	Nodal
Endothelial	
CD31	PECAM-1
NOS3	Endothelial nitric oxide synthase, NOS III
TEK	TEK tyrosine kinase, Tie-2
CDH5	Cadherin 5, type 2; VE-cadherin
VEGF	Vascular endothelial growth factor
VWF	von Willebrand factor/factor VIII-related antigen
Trophoblast	
GATA3	GATA-binding protein-3
HEY1	Hairy/enhancer-of-split related with YRPW motif 1
Miscellaneous	
EPO	Erythropoietin
HIF1A	Hypoxia inducible factor-1α
FST	Follistatin
SMAD1	Smad1
SMAD2	Smad2
SMAD3	Smad3
TGFB1	Transforming growth factor-β1
Control	
18S	

[a] This lists 47 genes representing markers of pluripotence, the three germ layers (ectoderm, mesoderm, and endoderm), endothelium, trophoblast, hypoxia, the TGFβ signaling pathways, and 18S endogenous control. Two genes, *FGF5* and *CD45*, did not amplify and were excluded from the analysis.

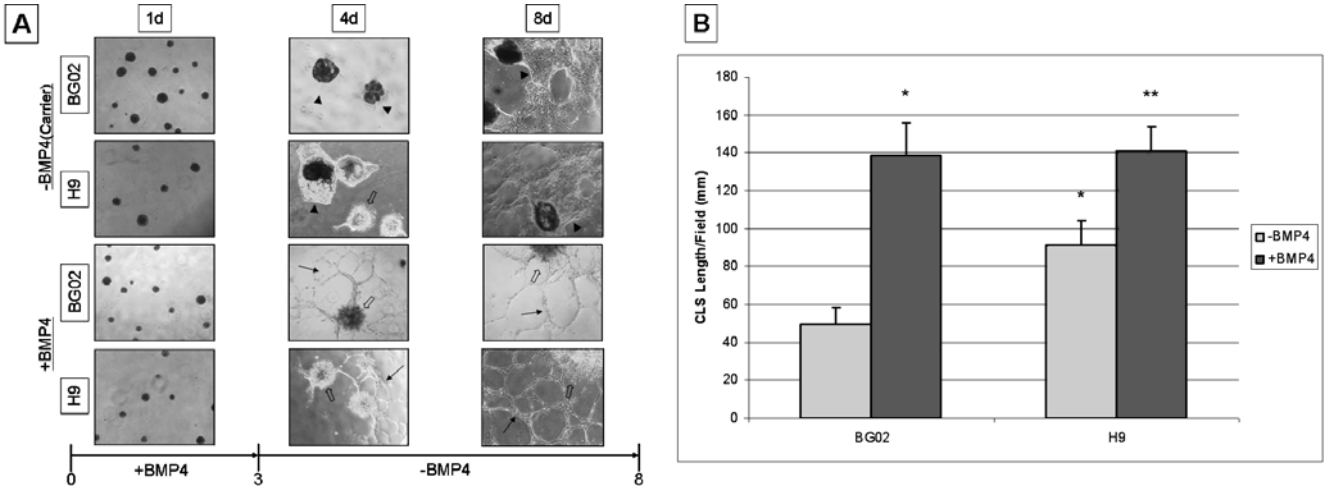

Figure 1. BMP4 treatment regulates network structure outgrowth. hESC lines BG02 and WA09 were manually passaged onto Matrigel and cultured in EGM-2 with either 100 ng/ml of BMP4 (+BMP4, bottom two rows) or an equivalent volume of control (–BMP4, top two rows) for 3 days. After 3 days, all cells were cultured in EGM-2 alone for another 5 days. (A) Phase contrast images were taken on Days 1 (left column), 4 (middle column), and 8 (right column) at ×4 magnification. hESC form EB and adhere to the Matrigel (1 day). After 3 to 4 days, cells begin to migrate out of the EB as sheets along the surface or into the gel (4 days). Treatment with BMP4 inhibits the cell sheets and increases the outgrowth of network structures. After 8 days, cell sheets, gel-invasive cells, and networks form in the control dishes while gel invasive cells and an extensive network characterizes BMP4-treated cultures (arrow head = migrating cell sheet; open arrow = gel invasive cells; thin arrow = network structures) (B) Network structure length was measured within a field and quantified using a Student's *t* test. WA09 control produced more network outgrowths compared with BG02 control (* $P < 0.05$). BMP4 statistically significantly increased the total network length compared with controls in both BG02 (* $P < 0.05$) and WA09 (** $P < 0.05$).

migration of a sheet of epithelial-like cells along the surface of the gel (Fig. 1A, 4d, arrowhead). By Day 8, the EB structures began to flatten because of mass migration of cells out onto the gel (Fig. 1A, 8d, arrowhead). When left to grow to confluence, a multilayered arrangement filled the culture dish (data not shown). In addition to the sheet morphology, cells from the EB invaded the three-dimensional gel with extended philopodia in a radial projection from the EB (Fig. 1A, 4d, and 8d, open arrow). When viewed with light projected from below (dissecting microscope), the cell sheets became transparent and allowed visibility of the gel invasive cells (data not shown). There was also an outgrowth of cells forming a network, similar in appearance to the capillary-like structures (CLS) formed by endothelial cells on Matrigel in an angiogenesis assay (Fig. 1A, 4d, and 8d, thin arrow). The EB formed by BG02 began to diminish in size when exposed to BMP4 compared with control, with the cell sheet migration generally inhibited while the gel invasive cells remained (Fig. 1A, 4d, and 8d, open arrow). BMP4 supplementation was also characterized by an increase in the network outgrowth and formation. When BMP4 addition ended at Day 3, some sheet formation occurred but was typically not as dense or expansive as seen in the control-treated dishes. In contrast, WA09-derived EB exposed to BMP4 maintained a relatively uniform size compared with control and did not experience shrinkage. There was a greater incidence of sheet outgrowth but not at the same level as BG02 control. In the same fashion, BMP4-treated WA09 cells demonstrated an increase in network formation and outgrowth compared with control (Fig. 1A).

To determine if BMP4 treatment quantifiably increased network formation we measured the total network length per field on Day 6 (BG02, $n = 6$, average number of fields = 10; WA09, $n = 5$, average number of fields = 11) (Fig. 1B). For BG02, there was an almost 3-fold increase in the total network outgrowth compared with control (Average ± SE: Control = 49 ± 9 mm vs. BMP4 = 139 ± 17 mm; $P < 0.05$). When comparing the effect of BMP4 on WA09 network outgrowth, we observed an approximately 1.5-fold, statistically significant increase (Average ± SE: Control = 92 ± 13 mm vs. BMP4 = 141 ± 13 mm; $P < 0.05$). It is interesting to note WA09 control also produced more network outgrowth than BG02 control ($P < 0.05$). As already mentioned, BG02 control predominantly produces a sheet of cells that migrate onto the gel surface before networks are typically seen. While WA09 control also has cell sheet migration, it was to a lesser extent than BG02. These results indicate BMP4 augments the formation and outgrowth of network structures in both BG02 and WA09 hESC. It also suggests individual cell lines may have subtle inherent differences making them more or less responsive to experimental conditions.

To determine if inhibition of BMP4 would block the outgrowth of the networks, we treated cultures with the BMP4 antagonist Noggin. For both BG02 and WA09, cultures were treated with equal volumes of BMP4 and Noggin controls, BMP4 (100 ng/ml) and Noggin control or BMP4 (100 ng/ml) and Noggin (300 ng/ml) for 3 days, then cultured for another 3 days in EGM-2 alone. As shown in Figure 2, the addition of Noggin completely blocked the effect of BMP4 on the EB. It is interesting to note the inhibition was so complete that the Noggin-treated cultures

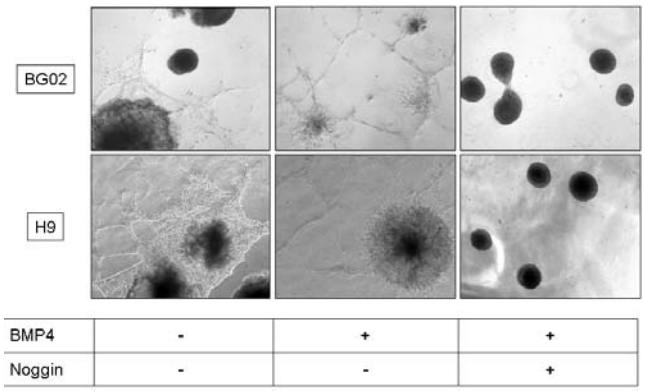

Figure 2. Noggin inhibits differentiation and network outgrowth. BG02 and WA09 were treated with BMP4 and Noggin controls (left column), 100 ng/ml BMP4 and Noggin control (middle column), or 100 ng/ml BMP4 and 300 ng/ml Noggin (right column) for 3 days, then EGM-2 alone for another 3 days. Noggin inhibited differentiation and network outgrowth in both cell lines (×4 magnification).

showed little change in EB morphology or cell migration. This suggests that not only was the effect of the supplemented BMP4 blocked, but differentiation cues inherent to the EGM-2 and Matrigel substrate were also blocked.

BMP4 Induction of Gene Expression in BG02 and WA09 hESC. We next wanted to determine the effect of BMP4 on temporal gene expression of endothelial as well as other markers of hESC differentiation. We utilized a qRT-PCR low-density array of 47 genes and 18S endogenous control. Genes were selected to monitor the state of pluripotence, the three germ layers (ectoderm, mesoderm, and endoderm), endothelium, trophoblast, transforming growth factor (TGF)β and bone morphogenetic (BMP) pathways, and hypoxia (Table 1). Manually passaged BG02 or WA09 were cultured as described with 100 ng/ml BMP4 or control with samples taken for RNA isolation on Days 0, 2, 4, 6, and 8 ($n = 3$ for both BG02 and WA09) and analyzed for statistical significance as described in the Materials and Methods. Two genes (*FGF5* and *CD45*) did not amplify and therefore were not considered in this analysis (raw data can be found at http://www.biomed.uga.edu/stice.html).

The first step of the statistical analysis was to determine the significance levels for the treatment, time, and the interaction between treatment and time. For BG02 and WA09, treatment was found to be significant in 24/45 (53%) and 15/45 (33%), time was significant in 28/45 (62%) and 28/45 (62%), and the combined effect of treatment and time was significant for 10/45 (22%) and 4/45 (9%), respectively, out of the genes surveyed. All of the pluripotent genes except *EBAF* for BG02 and *FOXA2* for WA09 were significantly downregulated with time, while 5/9 for BG02 and 3/9 for WA09 were significantly affected by BMP4 treatment (Fig. 3A). It has been shown by others that under specific conditions, BMP4 can induce WA09 to differentiate toward a global trophoblast phenotype (15). Here, two trophoblast markers were upregulated in this culture system for BG02 and WA09. BMP4 treatment induced a significant increase in expression of *HEY1* (Fig. 3B) in both cell types (BG02: treatment, $P < 0.001$; time, $P < 0.05$; treatment*-time interaction, $P < 0.05$; H9: treatment, $P < 0.05$) and *GATA3* (Fig. 3C) in BG02 (treatment, $P < 0.05$). Although *GATA3* was also upregulated in WA09, the difference was not significant. Ectoderm markers for BG02 and WA09 were all significantly affected by time with all but *FN1* (fibronectin) and *NESTIN* being downregulated (Fig. 3B). All of the BG02 ectoderm markers and *SOX2* for WA09 (Fig. 3C) were significantly affected by BMP4 treatment. For the three endoderm markers (*AFP*, *CER1*, and *HNF4A*) in this study, the only statistical significance was found in *AFP* (BG02 and WA09: $P < 0.05$) and how time affects its gene expression. We saw the largest relative upregulation with *AFP* compared with any other gene. Immunostaining detected small clusters of AFP^+ cells within the differentiating EB but absent in the network outgrowths (data not shown).

Because our interest was to examine gene expression profiles affecting endothelial differentiation, we focused on mesoderm and endothelial markers. Of the 15 mesoderm markers, GLM analysis indicated significant differences for BG02 and WA09, respectively, between the treatment (7 vs. 6) and time (8 vs. 7); only two genes from BG02 and none for WA09 demonstrated a combined effect of time and treatment. BRACHYURY expression reached a maximum at 2 days for both cell lines before declining to subbasal levels. In both cases, the control maximum expression was greater than BMP4 treatment, although a statistical difference was detected only in WA09. For both cell lines, genes for which one or more effects in the models were significant, LSMEANS contrasts between the different effect levels were inspected. For BG02, *ACVR1C*, *BMPR2*, *GATA4*, *KDR*/*Flk1*, *NODAL*, and *RUNX1* were significantly differentially expressed, while for WA09, *ACVR1B*, *BMPR2*, *CD34*, and *RUNX1* indicated differential regulation for BMP4 treatment as well as some treatment and time interactions (Fig. 3D). In some cases, GLM analysis indicated treatment was statistically different, but no difference was determined for the time points by LSMEANS analysis (e.g., WA09: *GATA4* and *NKX2–5*). KDR/Flk1 is the earliest known marker of cells capable of forming vascular progenitors (20). In both BG02 and WA09, *KDR* was upregulated, but only in BG02 at Day 4 did BMP4 induce statistically significant gene expression (Fig. 3E). Many of the genes associated with cardiovascular and hematopoietic development were increased under these culture conditions, though overall BMP4 treatment did not appear to influence their expression. This suggests mesoderm and its downstream products are produced in this system but of the genes monitored here, perhaps only *BMPR2* and *RUNX1* play a role in network formation and outgrowth.

For the endothelial markers, we observed an overall

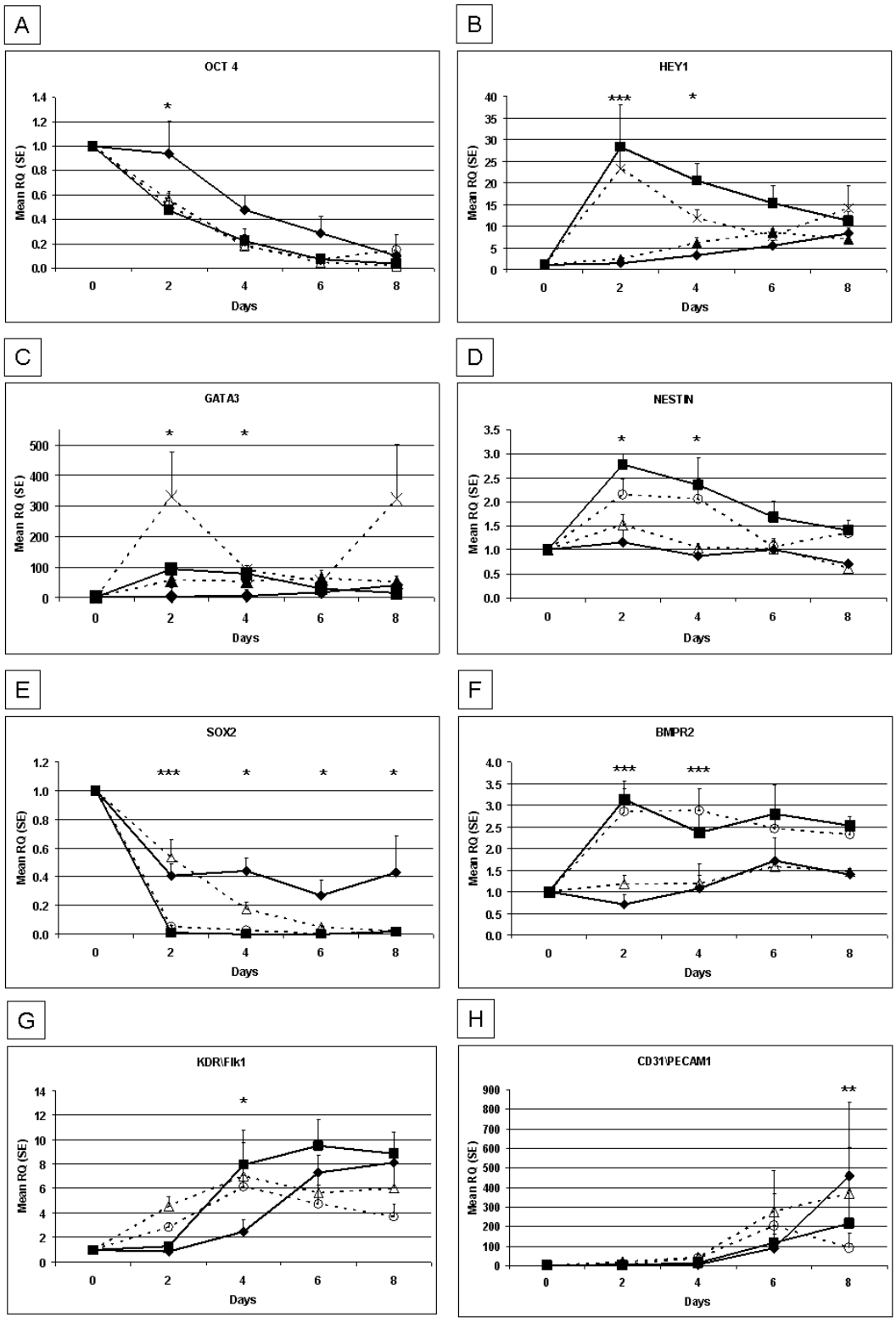

Figure 3. Least-squared mean gene expression analysis of BMP4 versus control time course for BGO2 and WA09. BG02 (solid lines) and WA09 (dashed lines) were cultured for 3 days ± BMP4, then for another 5 days in EGM-2 only. Samples were collected on Days 0, 2, 4, 6, and 8; total RNA was extracted, and gene expression was analyzed by qRT-PCR. Least-squared mean comparison was then expressed as *x*-fold change with respect to Day 0 control. The gene expression time course for (A) OCT4, (B) HEY1, (C) GATA3, (D) NESTIN, (E) SOX2, (F) BMPR2, (G) KDR/Flk1, and (H) CD31/PECAM1 are shown. (BG02: −BMP4 = solid diamond; +BMP4 = solid square; WA09: −BMP4 = open triangle; +BMP4 = open circle; * $P < 0.05$ for BG02 only; ** $P < 0.05$ for WA09 only; *** $P < 0.05$ for both BG02 and WA09).

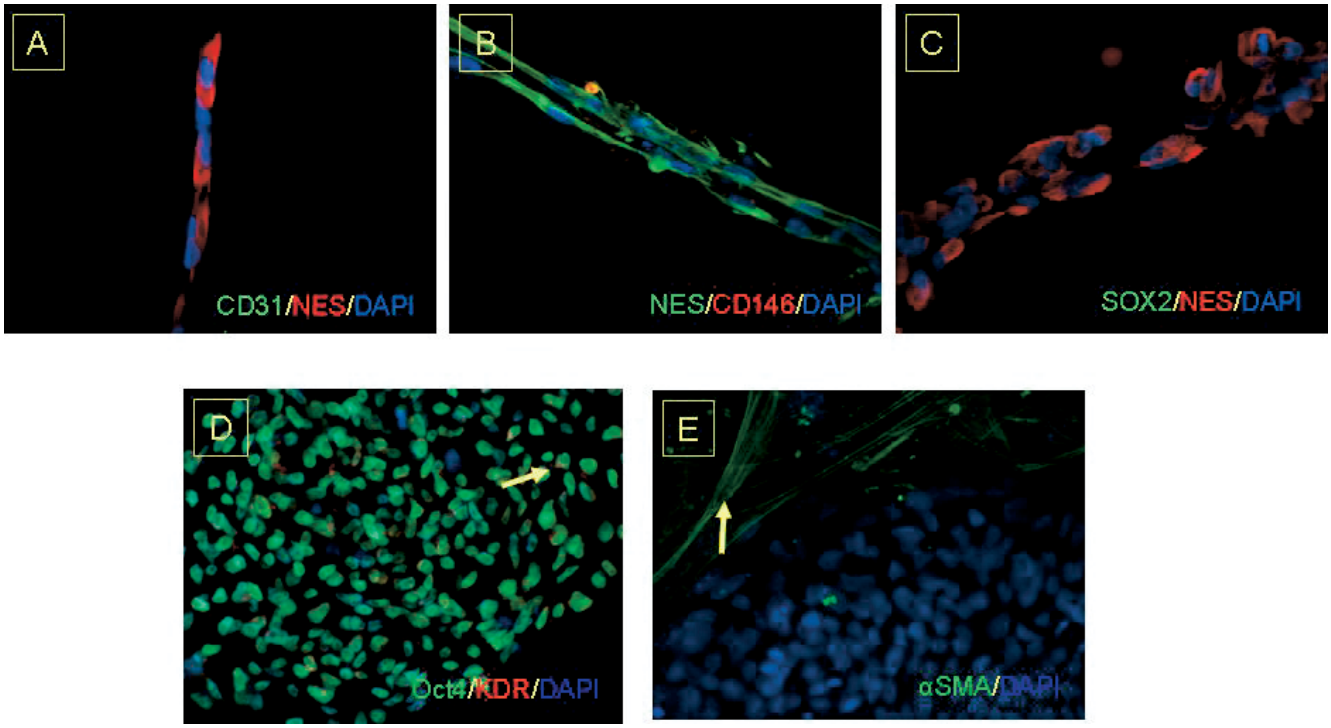

Figure 4. Network structures are CD31^{-}, CD146^{-}, and SOX2^{-}, and NESTIN^{+} while pluripotent cells are Oct4^{+}, KDR^{low}, and αSMA^{-}. Cultures were grown on glass-bottom dishes or chamber slides as described. To examine the expression of the common endothelial markers, cells were stained with (A) CD31 (green), (B) CD146 (red), or (C) SOX2 (green). All cultures were dual-immunostained with NESTIN (red in [A] and [C], green in [B]) and the nucleus counterstained with DAPI. Undifferentiated pluripotent cells were grown on MEFs and stained for (D) Oct4 (green) and KDR (red, indicated with arrow) or (E) αSMA (green, indicated with arrow), then counterstained with DAPI. All images were acquired with a ×40 oil objective, and a Z series stack was projected into a single image. A color figure is available in the online version of the journal.

robust upregulation for both cell lines with Tie-2/TEK and eNOS for BG02 and CD31/PECAM1 and vWF for WA09 showing differential expression with BMP4 treatment. CD31/PECAM1 is often used as a marker for mature endothelial cells and has been used for isolating hESC derived endothelial cells (21). In our model, we saw a large increase in CD31 gene expression for both cell lines with a statistically significant difference in expression for WA09 at Day 8 (Fig. 3F). However, we were not able to detect CD31^{+} cells by immunofluorescence in either the EB cell mass or network structures (Fig. 4A). Together, the gene expression data suggests the culture conditions are conducive to differentiation of hESC toward an endoderm and mesoderm phenotype at the expense of ectoderm and may be producing vascular components that assemble into the network structures seen here.

Vascular Marker Expression Within Residual EB and Networks. When examining the formation and growth of vascular structures, several markers are typically used for endothelial (CD31, KDR, and CD146) and smooth muscle (αSMA) identification. Since the outgrowth and network formation resembled that formed by endothelial cells in an angiogenesis assay, we initially used CD31 and CD146 for spatial localization of endothelial cells within the culture and to confirm the network composition. However, we were unable to detect either marker anywhere within the network structures or residual EBs (Fig. 4A and B) in spite of our ability to detect CD31^{+} and CD146^{+} HUVEC under the same conditions (data not shown). As was already mentioned, endothelial cells of the developing vascular system are positive for NESTIN (22), an intermediate filament originally associated with neural stem cells (23). Although negative for both CD31 and CD146, the networks and much of the residual EB were positive for commonly used neural marker NESTIN (Fig. 4A–C). However, we were unable to detect expression of the early neural and pluripotent marker SOX2 (Fig. 4C).

In the mouse, one of the earliest vascular markers is the VEGF-R2 or KDR (human)/Flk1 (mouse) (24). Yamashita *et al.* (20) showed Flk1^{+} mouse progenitor cells can differentiate into both endothelial and smooth muscle cells. In human hESC, KDR transcripts have been shown (25, 21), though to our knowledge protein expression has not. In Figure 4D, we show hESC grown on a MEF feeder layer that is dual-labeled for the pluripotent marker Oct4 (green) and KDR (red). Virtually the entire colony is Oct4-positive; while some KDR expression is detected within the colony (arrow), it does not appear to be globally expressed in undifferentiated cells. αSMA (Fig. 4E) is expressed in the surrounding MEF feeders (arrow) but not within the stem cell colony, in agreement with the findings of Huang *et al.* (26). Therefore, to identify the network-forming cells in our

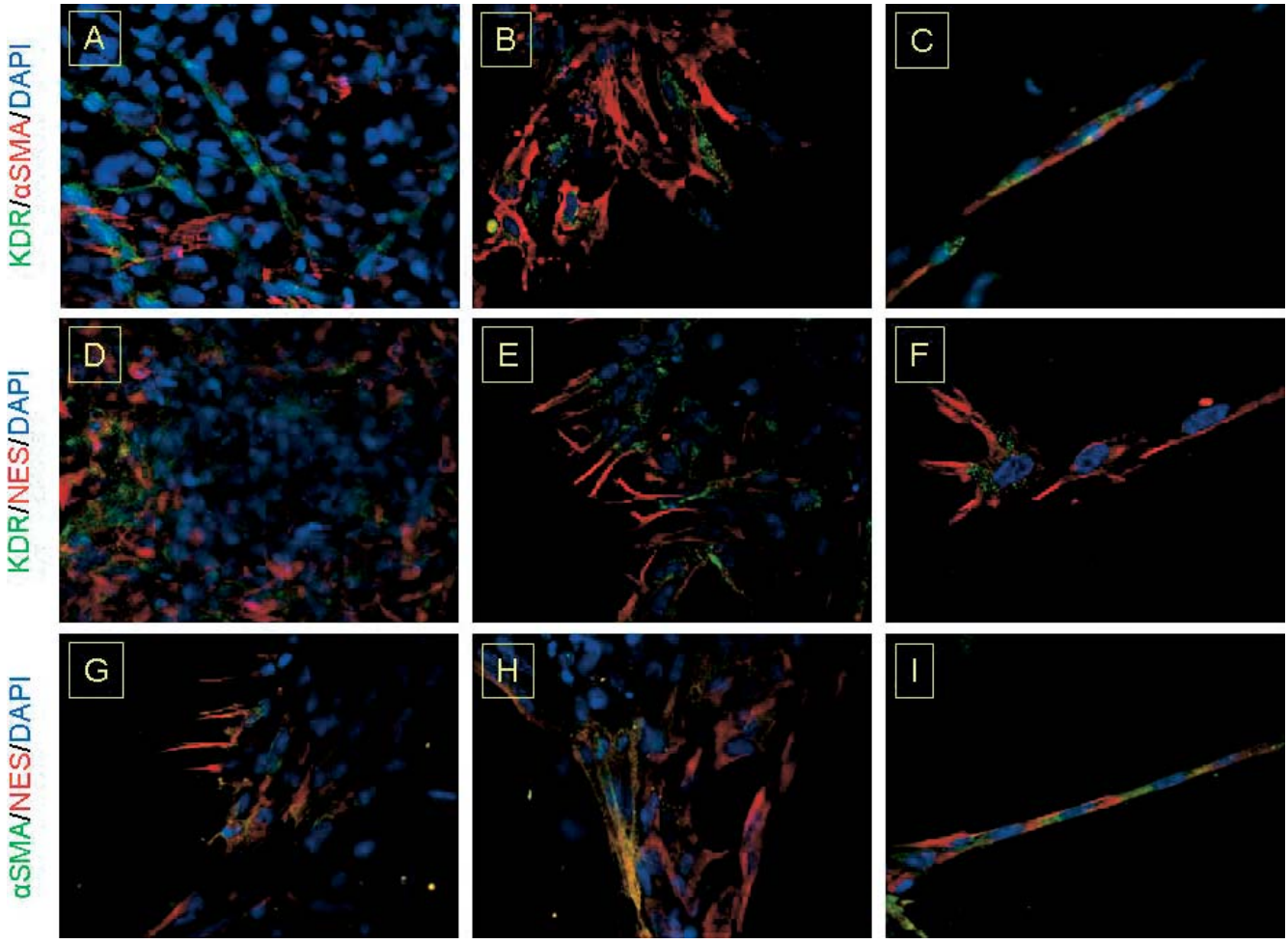

Figure 5. Early vascular markers KDR, αSMA, and NESTIN are detected within the network structures and elsewhere. Cell cultures were dual-immunostained to detect co-expression of KDR with αSMA (A–C), KDR with NESTIN (D–F), or αSMA with NESTIN (G–I), and the nucleus was counterstained with DAPI. For each case, three different morphologic regions were represented: the residual EB (A, D, and G), the periphery of the EB (B, E, and H), and the thin network structures (C, F, and I). All images were acquired with a ×40 oil objective, and a Z series stack was projected into a single image. A color figure is available in the online version of the journal.

culture, we used antibodies specific for KDR, αSMA, and NESTIN (Fig. 5). Within the residual EB, most cells were $NESTIN^{-}$ with some randomly arranged KDR^{+} and αSMA^{+} cells (Fig. 5A and D). Along the periphery all three proteins were detected with αSMA and NESTIN colocalizing in some cells (Fig. 5D and G). Where cells were migrating out of the EB, there was a higher incidence of KDR^{+} and αSMA^{+} where organized outgrowths appeared (Fig. 5B, E, and H). KDR does not specifically colocalize with the two cytoskeletal proteins as indicated by distinct staining patterns, but this could be a matter of where in the cell αSMA and NESTIN are expressed (Fig. 5B and E). As would be expected in cells expressing both proteins, NESTIN and αSMA were seen to colocalize in the same cells (Fig. 5H). In the small diameter networks, most cells were positive for NESTIN and many, but not all, for KDR or αSMA (Fig. 5C, F, and I). Where thin structures stretched across the gel and interconnected, an interesting pattern of protein segmentation was often seen (Fig. 5C and I). This could indicate compartmentalization of proteins within cells expressing both of the markers or different cell types individually expressing these proteins and combining to form a structure. In other instances, both proteins were expressed distinctly by the same cell, as in the case of the leading migratory cell in Figure 5F. Detection of the early vascular markers KDR, αSMA, and NESTIN, coupled with the lack of expression of the mature endothelial markers CD31 and CD146, suggest the network structures formed in this culture could be an immature vascular network.

Discussion

The main and novel findings in this study are (i) exposure of hESC to BMP4 increases the formation and outgrowth of network structures onto Matrigel; (ii) hESC (BG02 and WA09) differentiated in EGM2 on Matrigel show a rapid downregulation of pluripotent genes with a robust increase in endothelial marker genes and differential expression of BMPR2 and RUNX1 with BMP4 treatment;

and (iii) network structures are composed of cells negative for the endothelial markers CD31 and CD146, the neural marker SOX2, while positive for KDR, NESTIN and αSMA.

The effects of BMP4 on development have been well documented in multiple species including mouse, chick, zebrafish, and Xenopus (6, 27–29). One of the primary morphogenic functions of BMP4 is the induction of mesoderm (9, 30). Recently, Xu and colleagues (15) showed BMP4 induces hESC grown in a feeder-free culture system to preferentially form trophoblast gene expressing cells. Therefore, it is unclear what role BMP4 plays in vascular development in humans. Here, we have differentiated two hESC lines, WA09 and BG02, on Matrigel in EGM2 and show BMP4 exposure statistically significantly increases the formation and outgrowth of a network of cells. We specifically chose 100 ng/ml of BMP4 to parallel the dosage used by Xu *et al.* (15). Being a morphogen, BMP4's cellular effect is dose dependent, with higher exposure being associated with blood formation in Xenopus (31). The increase in network outgrowth with high-dose BMP4 treatment may indicate its morphogenic effect in human vascular development. Matrigel is a basement membrane composed primarily of type IV collagen, laminin, and heparin sulfate derived from Engelbreth-Holm-Swarm tumors and contains endogenous growth factors (e.g., bFGF, PDGF, EGF, NGF, IGF-1, and TGF-β), some of which play a role in endothelial and smooth muscle differentiation from progenitors (32). Here these factors may play a role in formation or supporting the viability of the networks. However, the BMP4-induced quantifiable increases in network outgrowth and Noggin inhibition of differentiation and lattice assembly suggests BMP4 signaling, or lack thereof, can modulate this process. Although both cell lines produced more network outgrowth with exposure to BMP4, we noted differences between them. Between untreated controls, H9 cultures produces significantly greater network outgrowth compared to BG02. In addition, treatment with BMP4 induced the BG02 colonies to shrink and inhibited the epithelial sheet migration, a phenomenon not noted as dramatically in H9. The reasons for this differential response are unknown but could be related to differences between the two cell lines or the initial culture conditions making them more or less responsive to experimental conditions.

Relative qRT-PCR was used to identify trends of differentiation within the culture towards all germ lineages. As expected, all of the pluripotent genes were downregulated as the cells began to differentiate. For those genes selected to monitor ectoderm, all markers were significantly downregulated with BMP4 treatment with the exception of NESTIN and FN1, which were transiently upregulated by BMP4 in the BG02 cell line. Although statistical differences were not found in WA09 control and BMP4-treated cultures, the trends in gene expression paralleled BG02. Of interest to these experiments is the association of both NESTIN and fibronectin to the vasculature. Fibronectin has been shown to be required for vascular assembly (33), while NESTIN is detected in developing endothelium (22), in mature capillary endothelium, and in angiogenic endothelial cells (34, 22). Although no difference was seen between control and BMP4 treatment in the endoderm markers, all three showed increases in expression over time. Endoderm signals to adjacent mesoderm and plays a role in regulating vascular development (35). AFP expression has been correlated with increased vascularization in tumors (36, 37) and as an angiogenic factor (38). The high AFP and general increase in endoderm gene expression could indicate a role in regulating cell specification leading to network formation.

For the two trophoblast markers included in this study, both showed early gene expression response to BMP4 treatment (15). This could indicate the formation of trophoblast lineages in addition to network outgrowths, possibly modeling an endothelial-like phenotype they assume when making the heterotypic endovascular placental-maternal connection (39, 40). Whether this represents extraembryonic or embryonic vasculogenesis is still to be determined.

Since we were specifically interested in vascular differentiation and development, we primarily examined genes of the mesoderm or endothelial lineage. Most of the genes followed were upregulated within this culture, but only BMPR2, a BMP4 receptor (41), and RUNX1, a transcription factor that binds BMP4-induced Smads and is involved in hematopoietic differentiation (42), were differentially regulated by BMP4 in both hESC lines. This suggests the effects seen with BMP4 treatment may be due to upregulation of the BMP4-signaling pathway and transcriptional regulation through RUNX1. Endothelial gene expression was altered by culture conditions but not further affected by the addition of BMP4. CD31 relative gene expression on Day 8 ranged from an approximate 70-fold to almost 500-fold increase when normalized to the Day 0 control. Despite this large increase, we were unable to detect CD31 protein expression. This suggests that although the relative increase in mRNA is large, the detection of CD31 by immunocytochemistry may lag behind the detected gene expression, and longer culture periods may produce CD31 positive cells. Alternatively, the actual number of copies may not be biologically significant, or posttranslational regulation prevents protein detection within the time course of this experiment.

We observed the network morphology and large increases in the mRNA of several endothelial markers and expected to be able to detect mature endothelial cells within the cultures by Day 8. Levenberg *et al.* (21) utilized CD31 for sorting differentiated cells (potential endothelial cells) from 8-day EB. However, Kaufman *et al.* (43) were unable to detect CD31 when differentiating Rhesus monkey ES to endothelial cells and hence used CD146 for 29 days of their differentiation protocol. We, however, were unable to detect

either CD31 or CD146. The lack of mature endothelial markers and expression of NESTIN suggested the possibility the observed structures were of nonendothelial lineage. However, the intermediate filament NESTIN is expressed in the developing vasculature, capillaries, and angiogenic endothelial cells (22, 34). Also, immunocytochemical analyses by others have indicated mouse ES–derived endothelial cells do not express all markers at the same level as primary cultured mouse aortic endothelial cells and therefore may still be an immature phenotype (44). In support of this, we were able to detect VEGF-R2 or KDR, αSMA as well as NESTIN. KDR is embryonic lethal in the null mouse (45) and is the earliest known marker of vascular-hematopoietic lineage (20), while αSMA is a common marker for smooth muscle cells (46). Although several possibilities exist as to what these network structures represent, the lack of mature and abundance of early endothelial and smooth muscle markers suggest this could be an immature vascular network. If so, it appears these cells are able to migrate and assemble into structures recapitulating vasculogenesis without expressing the more common vascular markers. A third possibility is the co-development of vascular and neural structures. Recent research demonstrates the parallel growth patterns and molecular cues regulating neurovascular development (47). Further work to identify the nature of gene expression in these structures will enable precise identification and lead to insights into their development and functionality.

These findings confirm the use of stem cells and the EB as a model of early development including vasculogenesis (3, 4). Using hESC in this manner can provide insights into the mechanisms regulating the earliest events in human vasculogenesis. An understanding of how the vasculature is formed could also be applied to tissue engineering and angiogenic/ischemic therapies.

We thank R. Nilsen for help with the qRT-PCR.

1. Jain RK. Molecular regulation of vessel maturation. Nat Med 9:685–693, 2003.
2. Itskovitz-Eldor J, Schuldiner M, Karsenti D, Eden A, Yanuka O, Amit M, Soreq H, Benvenisty N. Differentiation of human embryonic stem cells into embryoid bodies compromising the three embryonic germ layers. Mol Med 6:88–95, 2000.
3. Feraud O, Cao Y, Vittet D. Embryonic stem cell-derived embryoid bodies development in collagen gels recapitulates sprouting angiogenesis. Lab Invest 81:1669–1681, 2001.
4. Risau W, Sariola H, Zerwes HG, Sasse J, Ekblom P, Kemler R, Doetschman T. Vasculogenesis and angiogenesis in embryonic-stem-cell-derived embryoid bodies. Development 102:471–478, 1988.
5. Baron MH. Molecular regulation of embryonic hematopoiesis and vascular development: a novel pathway. J Hematother Stem Cell Res 10:587–594, 2001.
6. Winnier G, Blessing M, Labosky PA, Hogan BL. Bone morphogenetic protein-4 is required for mesoderm formation and patterning in the mouse. Genes Dev 9:2105–2116, 1995.
7. Jones CM, Lyons KM, Lapan PM, Wright CV, Hogan BL. DVR-4 (bone morphogenetic protein-4) as a posterior-ventralizing factor in Xenopus mesoderm induction. Development 115:639–647, 1992.
8. Chadwick K, Wang L, Li L, Menendez P, Murdoch B, Rouleau A, Bhatia M. Cytokines and BMP-4 promote hematopoietic differentiation of human embryonic stem cells. Blood 102:906–915, 2003.
9. Johansson BM, Wiles MV. Evidence for involvement of activin A and bone morphogenetic protein 4 in mammalian mesoderm and hematopoietic development. Mol Cell Biol 15:141–151, 1995.
10. Li F, Lu S, Vida L, Thomson JA, Honig GR. Bone morphogenetic protein 4 induces efficient hematopoietic differentiation of rhesus monkey embryonic stem cells in vitro. Blood 98:335–342, 2001.
11. Zou H, Niswander L. Requirement for BMP signaling in interdigital apoptosis and scale formation. Science 272:738–741, 1996.
12. Song Q, Mehler MF, Kessler JA. Bone morphogenetic proteins induce apoptosis and growth factor dependence of cultured sympathoadrenal progenitor cells. Dev Biol 196:119–127, 1998.
13. Okamoto M, Murai J, Yoshikawa H, Tsumaki N. Bone morphogenetic proteins in bone stimulate osteoclasts and osteoblasts during bone development. J Bone Miner Res 21:1022–1033, 2006.
14. Xu RH, Peck RM, Li DS, Feng X, Ludwig T, Thomson JA. Basic FGF and suppression of BMP signaling sustain undifferentiated proliferation of human ES cells. Nat Methods 2:185–190, 2005.
15. Xu RH, Chen X, Li DS, Li R, Addicks GC, Glennon C, Zwaka TP, Thomson JA. BMP4 initiates human embryonic stem cell differentiation to trophoblast. Nat Biotechnol 20:1261–1264, 2002.
16. Mitalipova M, Calhoun J, Shin S, Wininger D, Schulz T, Noggle S, Venable A, Lyons I, Robins A, Stice S. Human embryonic stem cell lines derived from discarded embryos. Stem Cells 21:521–526, 2003.
17. Levenstein ME, Ludwig TE, Xu RH, Llanas RA, VanDenHeuvel-Kramer K, Manning D, Thomson JA. Basic fibroblast growth factor support of human embryonic stem cell self-renewal. Stem Cells 24: 568–574, 2006.
18. Livak KJ, Schmittgen TD. Analysis of relative gene expression data using real-time quantitative PCR and the 2(-Delta Delta C(T)) Method. Methods 25:402–408, 2001.
19. Debnath J, Muthuswamy SK, Brugge JS. Morphogenesis and oncogenesis of MCF-10A mammary epithelial acini grown in three-dimensional basement membrane cultures. Methods 30:256–268, 2003.
20. Yamashita J, Itoh H, Hirashima M, Ogawa M, Nishikawa S, Yurugi T, Naito M, Nakao K, Nishikawa S. Flk1-positive cells derived from embryonic stem cells serve as vascular progenitors. Nature 408:92–96, 2000.
21. Levenberg S, Golub JS, Amit M, Itskovitz-Eldor J, Langer R. Endothelial cells derived from human embryonic stem cells. Proc Natl Acad Sci U S A 99:4391–4396, 2002.
22. Mokry J, Cizkova D, Filip S, Ehrmann J, Osterreicher J, Kolar Z, English D. Nestin expression by newly formed human blood vessels. Stem Cells Dev 13:658–664, 2004.
23. Lendahl U, Zimmerman LB, McKay RD. CNS stem cells express a new class of intermediate filament protein. Cell 60:585–595, 1990.
24. Nishikawa SI, Nishikawa S, Hirashima M, Matsuyoshi N, Kodama H. Progressive lineage analysis by cell sorting and culture identifies FLK1+VE-cadherin+ cells at a diverging point of endothelial and hemopoietic lineages. Development 125:1747–1757, 1998.
25. Kaufman DS, Hanson ET, Lewis RL, Auerbach R, Thomson JA. Hematopoietic colony-forming cells derived from human embryonic stem cells. Proc Natl Acad Sci U S A 98:10716–10721, 2001.
26. Huang H, Zhao X, Chen L, Xu C, Yao X, Lu Y, Dai L, Zhang M. Differentiation of human embryonic stem cells into smooth muscle cells in adherent monolayer culture. Biochem Biophys Res Commun 351:321–327, 2006.
27. Connolly DJ, Patel K, Withington S, Cooke J. Effects of follistatin and BMP4 proteins on early dorso-ventral patterning in chick. Int J Dev Biol 44:129–140, 2000.
28. Hammerschmidt M, Serbedzija GN, McMahon AP. Genetic analysis of

dorsoventral pattern formation in the zebrafish: requirement of a BMP-like ventralizing activity and its dorsal repressor. Genes Dev 10:2452–2461, 1996.
29. Fainsod A, Steinbeisser H, De Robertis EM. On the function of BMP-4 in patterning the marginal zone of the Xenopus embryo. EMBO J 13: 5015–5025, 1994.
30. Wiles MV, Johansson BM. Embryonic stem cell development in a chemically defined medium. Exp Cell Res 247:241–248, 1999.
31. Dale L. Pattern formation: a new twist to BMP signalling. Curr Biol 10: R671–R673, 2000.
32. Kleinman HK, Martin GR. Matrigel: basement membrane matrix with biological activity. Semin Cancer Biol 15:378–386, 2005.
33. George EL, Baldwin HS, Hynes RO. Fibronectins are essential for heart and blood vessel morphogenesis but are dispensable for initial specification of precursor cells. Blood 90:3073–3081, 1997.
34. Mokry J, Nemecek S. Angiogenesis of extra- and intraembryonic blood vessels is associated with expression of nestin in endothelial cells. Folia Biol (Praha) 44:155–161, 1998.
35. Dyer MA, Farrington SM, Mohn D, Munday JR, Baron MH. Indian hedgehog activates hematopoiesis and vasculogenesis and can respecify prospective neurectodermal cell fate in the mouse embryo. Development 128:1717–1730, 2001.
36. Koide N, Nishio A, Igarashi J, Kajikawa S, Adachi W, Amano J. Alpha-fetoprotein-producing gastric cancer: histochemical analysis of cell proliferation, apoptosis, and angiogenesis. Am J Gastroenterol 94: 1658–1663, 1999.
37. Peng SY, Chen WJ, Lai PL, Jeng YM, Sheu JC, Hsu HC. High alpha-fetoprotein level correlates with high stage, early recurrence and poor prognosis of hepatocellular carcinoma: significance of hepatitis virus infection, age, p53 and beta-catenin mutations. Int J Cancer 112:44–50, 2004.
38. Liang OD, Korff T, Eckhardt J, Rifaat J, Baal N, Herr F, Preissner KT, Zygmunt M. Oncodevelopmental alpha-fetoprotein acts as a selective proangiogenic factor on endothelial cell from the fetomaternal unit. J Clin Endocrinol Metab 89:1415–1422, 2004.
39. Zhou Y, Fisher SJ, Janatpour M, Genbacev O, Dejana E, Wheelock M, Damsky CH. Human cytotrophoblasts adopt a vascular phenotype as they differentiate. A strategy for successful endovascular invasion? J Clin Invest 99:2139–2151, 1997.
40. Damsky CH, Fisher SJ. Trophoblast pseudo-vasculogenesis: faking it with endothelial adhesion receptors. Curr Opin Cell Biol 10:660–666, 1998.
41. De Caestecker M. The transforming growth factor-beta superfamily of receptors. Cytokine Growth Factor Rev 15:1–11, 2004.
42. Ito Y, Miyazono K. RUNX transcription factors as key targets of TGF-beta superfamily signaling. Curr Opin Genet Dev 13:43–47, 2003.
43. Kaufman DS, Lewis RL, Hanson ET, Auerbach R, Plendl J, Thomson JA. Functional endothelial cells derived from rhesus monkey embryonic stem cells. Blood 103:1325–1332, 2004.
44. McCloskey KE, Smith DA, Jo H, Nerem RM. Embryonic stem cell-derived endothelial cells may lack complete functional maturation in vitro. J Vasc Res 43:411–421, 2006.
45. Shalaby F, Ho J, Stanford WL, Fischer KD, Schuh AC, Schwartz L, Bernstein A, Rossant J. A requirement for Flk1 in primitive and definitive hematopoiesis and vasculogenesis. Cell 89:981–990, 1997.
46. Bagley RG, Weber W, Rouleau C, Teicher BA. Pericytes and endothelial precursor cells: cellular interactions and contributions to malignancy. Cancer Res 65:9741–9750, 2005.
47. Carmeliet P, Tessier-Lavigne M. Common mechanisms of nerve and blood vessel wiring. Nature 436:193–200, 2005.